

Analysis of the polarization-dependent rate of associative ionization of radiatively excited Na(3p) atoms

Dumont M. Jones and John S. Dahler

Departments of Chemistry and Chemical Engineering, University of Minnesota, Minneapolis, Minnesota 55455

(Received 9 August 1984)

Kircz, Morgenstern, and Nienhuis [Phys. Rev. Lett. **48**, 610 (1982)] have measured the cross section for the associative ionization of partially oriented pairs of excited $[(3p)^2P_{3/2}]$ sodium atoms. Here, we extract information from these data about the identities of the participating adiabatic Born-Oppenheimer states of Na_2 . It is definitely established that more than one of these states is involved. The greatest contributor is the $X^1\Sigma_g^+$ state with the dominant molecular-orbital configuration σ_g^2 (at small internuclear separations). It is highly probable that only one other state (either the $^1\Sigma_g^+$ or $^3\Sigma_g^-$ state with the dominant molecular-orbital configuration π_u^2) is involved, but a small contribution from one state ($^1\Pi_u$ or $^3\Pi_u$) with the configuration $\sigma_g\pi_u$ cannot be unequivocally dismissed.

I. INTRODUCTION

Within the past few years there have been several experimental studies¹⁻⁵ of associative ionization (AI) resulting from collisions between two sodium atoms in 3p electronic states. In one of the most recent of these, Kircz, Morgenstern, and Nienhuis⁵ (KMN) measured the dependence of the rate of AI on the angle between the direction of relative motion of the colliding atoms and the polarization axis of the laser used to prepare the reactive $(3p)^2P_{3/2}$ state. Our objective here is to determine whether these data can be used to identify which quasimolecular states of Na_2 contribute to the observed rate of the AI process

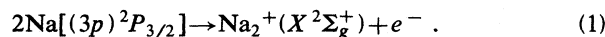


Figure 1 shows several potential-energy curves which are pertinent to this reaction. Those specific to the $X^1\Sigma_g^+[\text{Na}(^2P)-\text{Na}(^2P)]$ state of Na_2 and to the $X^2\Sigma_g^+$

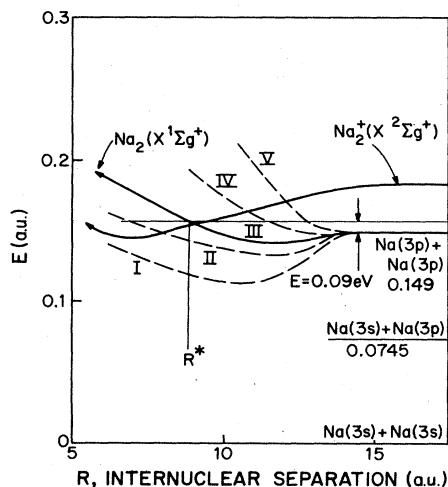


FIG. 1. Potential-energy curves for Na_2^+ and Na_2 (Ref. 6). Energies are given in atomic units, 1 a.u. = 13.6 eV. R^* indicates the classical turning point.

ground state of Na_2^+ were calculated by Montagnani, Riani, and Salvetti.⁶ Four others, labeled I, II, IV, and V, are included here for speculative purposes and do not correspond to any definitely known molecular states of Na_2 . In order for AI to occur, the turning point of the classical trajectory associated with the relative motion of two colliding atoms must be located at an internuclear separation for which the adiabatic Born-Oppenheimer (ABO) state of the reactants is degenerate with a continuum electronic state of the ionized configuration $\text{Na}_2^+(X^2\Sigma_g^+) + e^-$. In the experiments of KMN the collisions occur under thermal conditions so that the electronic transitions responsible for the observed diatomic product ions must be exoergic or at best only very weakly endoergic. Thus, in order to participate in the reaction an ABO state must have an electronic energy which resembles one of the curves labeled II, III, or IV in Fig. 1. States with potential-energy curves similar to I are stable with respect to AI and those with steeply repulsive curves similar to V only become reactive when the relative kinetic energy of the colliding atoms is greatly in excess of the thermal mean. Curve III calculated by Montagnani *et al.* suggests that the $X^1\Sigma_g^+$ state of Na_2 is a likely contributor to the thermal AI reaction. There are other ABO states which correlate asymptotically with the same atomic states ($^2P+^2P$) as does $X^1\Sigma_g^+$. Our goal is to establish which ABO states contribute to the thermal AI reaction. This we propose to accomplish with the aid of KMN's experimental data but without recourse to detailed electronic state calculations.

In the experiments of Kircz, Morgenstern, and Nienhuis (see Fig. 2) a collimated beam emerging from an effusive oven is crossed at right angles by a 100-mW laser tuned to the $F=2 \rightarrow F=3$ hyperfine transition of the Na D_2 line. This populates the substates of $\text{Na}(^2P_{3/2})$ in the ratio 1:5 for $|M_J| = \frac{3}{2}, \frac{1}{2}$. The projection quantum number M_J labels the component of total electronic angular momentum parallel to the polarization axis of the laser. The angle (β) between this axis and the direction of the atomic beam can be varied systematically.

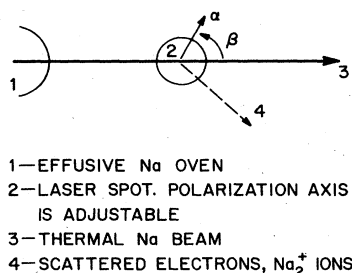


FIG. 2. Schematic depiction of the Kircz-Morgenstern-Nienhuis (Ref. 5) experiment. A detailed description is given in the text.

Due to axial dispersion within the beam some atoms move more rapidly than others and so collisions occur. Those which result in AI produce ions that can be collected and mass analyzed. At the low laser intensities used by KMN the probabilities for the occurrence of multiphoton absorption and of laser-induced associative ionization are negligible. Therefore, the only role played by the laser is that of populating the $^2P_{3/2}$ state of the beam atoms. Furthermore, the beam density is so low ($5 \times 10^8 - 5 \times 10^9$ particles/cm³) that collisional depolarization of this state does not occur. This means that the relative populations of the various magnetic substates are governed solely by the laser intensity. Finally, the spatial orientations of the

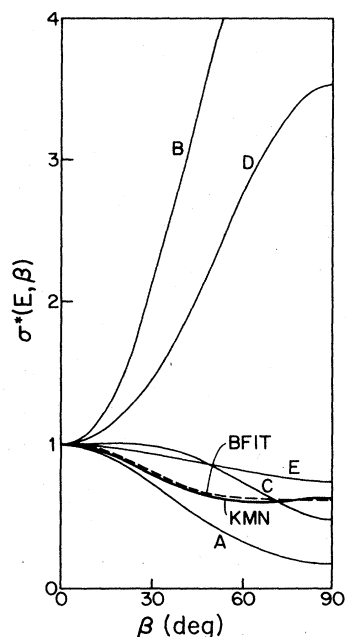


FIG. 3. Dimensionless cross section $\sigma^*(E, \beta)$ [$\equiv \sigma(E, \beta)/\sigma(E, 0)$] for associative ionization. The broadest of the solid curves, labeled KMN, gives the experimental results of Kircz, Morgenstern, and Nienhuis (Ref. 5). The curves labeled A, B, C, D, and E are plots of the dimensionless cross sections $\sigma_{\alpha\alpha}^*(E, \beta)$ specific to the individual ABO states $\alpha = A, B, C, D$, and E. Finally, the dashed curve labeled BFIT is the best fit gotten from the theoretical formula (20). It was obtained (see text for details) by setting $\sigma_{AA} \approx 23$, $\sigma_{CC} = \sigma_{EE} = 0$, and $\sigma_{BB} \approx 8.97 - 2.13\sigma_{DD}$, with $4 > \sigma_{DD} > 2.5$.

associated $3p$ orbitals are fixed by the laser's axis of polarization.

This control over the orientations of the $3p$ orbitals is a tool which can be used, at least in principle, to determine whether more than one ABO state contributes to the collisional production of diatomic ions: by rotating the polarization axis of the laser one can vary the relative populations of two or more competing reactant states. For example, some collisions will involve pairs of reactant atoms with their valence $3p$ orbitals aligned along the direction of the asymptotic relative motion (favorably oriented for the formation of $p\sigma$ molecular orbitals) while others will involve pairs with orbitals aligned perpendicular to this direction (and hence, favorably oriented for the formation of $p\pi$ orbitals). One can produce a bias in favor of the first of these configurations by aligning ($\beta=0$) the laser polarization with the beam axis, the latter of which is coincident with the asymptotic direction of relative motion of pairs of colliding atoms. A bias for the second configuration is produced by setting the laser polarization perpendicular ($\beta=\pi/2$) to the beam axis.

The darkest line in Fig. 3 is the KMN integral cross section for AI plotted as a function of β . This reaction rate varies substantially with the angle β , reaching a maximum with the beam and polarization axes coincident and falling to approximately 60% of this maximum when the beam and polarization axes are perpendicular. The remainder of this paper is devoted to the implications of these data with regard to identifying the reactive quasi-molecular states of Na₂, an issue which was addressed neither by KMN nor by Nienhuis.⁷

II. THEORY

The integral cross section specific to the production of diatomic Na₂⁺ ions in a single electronic state ($X^2\Sigma_g^+$ in the present case) is given by the formula⁸

$$\sigma(E, \beta) = \frac{M_e^2}{4\pi^2 \hbar^4} \text{Tr} \left[v_f T \left[\frac{1}{v} \rho \right] T^\dagger \right] \quad (2)$$

Here T is the transition operator for AI, v the relative velocity of the reactants Na+Na, M_e the reduced mass of the reaction products Na₂⁺+e⁻, and $v_f \equiv v(\epsilon) \equiv (2M_e \epsilon)^{1/2}$ the magnitude of their relative velocity. The trace operation Tr extends over all labels needed to characterize the final state, exclusive of the electron spin (multiplicity) and parity (g or u) of the product ion and the quantum number Λ_f (here equal to zero) which designates the component of electronic orbital angular momentum of this ion along its internuclear axis. The labels belonging to the trace set include the kinetic energy and direction of motion of the ejected electron [for which we adopt the notation $\vec{\epsilon} = (\epsilon, \hat{\epsilon})$] and a collection f consisting of the vibrational and rotational quantum numbers of the product ion and the quantum numbers for electron spin. Here and henceforth we neglect spin-orbit coupling so that electron spin and the internuclear component of electronic orbital angular momentum are separate constants of the motion.

The initial state of the atomic reactants is characterized

by a density operator ρ which can be written as a direct product

$$\frac{1}{v}\rho = \frac{1}{v}\rho_{\text{nuc}} \otimes \rho_{\text{el}} \quad (3)$$

of the two factors

$$\frac{1}{v}\rho_{\text{nuc}} = \int d\vec{k} |\vec{k}\rangle \left\langle \frac{P_{\text{nuc}}(\vec{k})}{v_k} \right\rangle \langle \vec{k}|, \quad v_k = \hbar |\vec{k}| / \mu \quad (4)$$

$$\rho_{\text{el}} = \sum_{M_A, M_B} |M_A, M_B\rangle P_{\text{el}}(M_A, M_B) \langle M_A, M_B|. \quad (5)$$

$P_{\text{nuc}}(\vec{k})$ is the distribution function associated with the relative momenta of colliding atomic pairs. It is strongly peaked in the direction of the beam axis and narrowly centered about a value $p = (2\mu E)^{1/2}$ defined in terms of the mean kinetic energy $E = \int d^3\vec{k} P_{\text{nuc}}(\vec{k}) (\hbar^2 k^2 / 2\mu)$ of the relative motion. The bras and kets, $\langle \vec{k}|$ and $|\vec{k}\rangle$, indicate plane-wave states.

The electronic density matrix given by Eq. (5) has the diagonal form appropriate to incoherently populated excited states. Off-diagonal elements would occur only if the duration of the laser pulse were comparable to the lifetime for spontaneous emission,⁹ vis. 10 ns. Because both atoms (labeled A and B) are in 2P states with $J = \frac{3}{2}$, we use the abbreviated notation $|J_j, M_j\rangle = |M_j\rangle$, $|J_A, M_A; J_B, M_B\rangle = |M_A, M_B\rangle$. The symbol $P_{\text{el}}(M_A, M_B)$ stands for the product $p_A(M_A)p_B(M_B)$ with $p_j(M_j)$ denoting the probability that the projection (along the polarization axis of the laser) quantum number of atom j equals M_j . The bras and kets, $\langle M_A, M_B|$ and $|M_A, M_B\rangle$, are antisymmetric states specific to two widely separated atoms. In the two-electron, valence-shell approximation they assume the simple forms

$$|M_A, M_B\rangle = 2^{-1/2} (|M_A\rangle |M_B\rangle - |M_B\rangle |M_A\rangle).$$

The cross section given by (2) can be rewritten in the more explicit form

$$\sigma(E, \beta) = \sum_{\alpha', \alpha''} \sigma_{\alpha'\alpha''}(E) \langle \alpha' | \rho_{\text{el}} | \alpha'' \rangle, \quad (6)$$

with the summations extending over complete sets of ABO electronic states and where

$$\sigma_{\alpha'\alpha''}(E) = \frac{M_e^2}{4\pi^2 \hbar^4} \int d\vec{k} \left\langle \frac{P_{\text{nuc}}(\vec{k})}{v_k} \right\rangle \times \sum_{\vec{e}, f} v_f \langle \langle f, \vec{e} | T | \alpha', \vec{k} \rangle \rangle \langle \langle \alpha'', \vec{k} | T^\dagger | f, \vec{e} \rangle \rangle \quad (7)$$

and

$$\langle \alpha' | \rho_{\text{el}} | \alpha'' \rangle = \sum_{M_A, M_B} \langle \alpha' | M_A, M_B \rangle P_{\text{el}}(M_A, M_B) \times \langle M_A, M_B | \alpha'' \rangle. \quad (8)$$

Here $\langle \langle f, \vec{e} | T | \alpha, \vec{k} \rangle \rangle$ is the matrix element of the transition operator which connects reactants in the ABO

state α and with relative momentum $\hbar\vec{k}$ to ionized products in states characterized by the previously defined labels f and \vec{e} . The selection rules for this operator place severe restrictions on the terms which contribute to the summations of Eq. (6). The nature and origin of these rules are revealed by an examination of the formula

$$\langle \langle f, \vec{e} | T | \alpha, \vec{k} \rangle \rangle = \int d\vec{R} [\Psi_f^M(E_n^L | \vec{R})]^* \langle \vec{e} | \vec{R} \rangle_\alpha \chi_\alpha^+(\vec{k} | \vec{R}) \quad (9)$$

derived by Bieniek.¹⁰ This formula incorporates the assumption that Born-Oppenheimer couplings are of negligible importance compared to the matrix elements

$$\langle \vec{e} | \vec{R} \rangle_\alpha = \int d\vec{r} [\phi_{\vec{e}}^-(\vec{r} | \vec{R})]^* H_{\text{el}} \phi_\alpha(\vec{r} | \vec{R}) \quad (10)$$

of H_{el} , the effective Hamiltonian operator for two valence electrons in the field of the Na^+ cores. $\phi_\alpha(\vec{r} | \vec{R})$ is the coordinate representation (\vec{r} for electrons, \vec{R} for nuclei) of the wave function for the ABO electronic state α and $\chi_\alpha^+(\vec{k} | \vec{R})$ is the nuclear wave function associated with this particular electronic state of the reactants. Similarly, $\phi_{\vec{e}}^-(\vec{r} | \vec{R})$ is the electronic wave function for the continuum state consisting of a diatomic ion and an unbound electron. This function $\phi_{\vec{e}}^-(\vec{r} | \vec{R})$ can be written as a linear combination

$$\sum_{\lambda, \mu} \{ [Y_{\lambda, \mu}(\hat{e})]_{\vec{R}} i^\lambda \exp(-i\sigma^\lambda) \} \phi_{\epsilon\lambda\mu}^-(\vec{r} | \vec{R}),$$

where $\phi_{\epsilon\lambda\mu}^-(\vec{r} | \vec{R})$ is an eigenfunction of the parity operator and of the projection of electronic orbital angular momentum along the internuclear axis (see Appendix). The superscripts $+$ and $-$ refer to functions which satisfy the conventionally defined "out" and "in" boundary conditions of scattering theory. Finally, $\Psi_f^M(E_n^L | \vec{R})$ is the wave function descriptive of the rotational (L, M) and vibrational (n) motions of a diatomic product ion with internal energy E_n^L .

Because H_{el} belongs to the identity representation of the diatomic group $D_{\infty h}$, the selection rules for $\langle \vec{e} | \vec{R} \rangle_\alpha$ are the same as those for the electronic overlap integral of $\phi_{\vec{e}}^-$ (or $\phi_{\epsilon\lambda\mu}$) and ϕ_α . These are the following.

(i) The total electronic spin and its projection are conserved: $S_\alpha = S_{\vec{e}}$ and $\Sigma_\alpha = \Sigma_{\vec{e}}$ (or $S_{z, \alpha} = S_{z, \vec{e}}$).

(ii) The projection of the total electronic orbital angular momentum along the internuclear axis is conserved. Thus, $\Lambda_\alpha = \Lambda_f + \mu$, with Λ_α denoting the projection quantum number of the initial ABO state α and Λ_f denoting that of the project diatomic ion. μ is the axial projection of the orbital angular momentum of the ejected electron.

(iii) The parities of the initial and final electronic states must be equal.

A more approximate but no less important selection rule is the previously stated requirement that

(iv) the classical turning point (R^*, E^*) must be located within the part of the R - E plane (cf. Fig. 1) associated with the electronic continuum of $\text{Na}_2^+ + e^-$. This (Franck-Condon) rule is a direct consequence of Eq. (9),

for unless the overlap between the nuclear wave functions $\Psi_f^M(E_n^L | \vec{R})$ and $\chi_\alpha^+(\vec{k} | \vec{R})$ is significant, the integral itself will be negligibly small.

There is a final selection rule which, like (iv), pertains to the nuclear degrees of freedom. It is a direct consequence of assuming (Franck-Condon principle) that the electronic transition does not alter the angular momentum associated with the relative motion of the two heavy particles (Na^+ cores). According to this selection rule (see Appendix)

(v) the transition matrix element $\langle\langle f, \vec{\epsilon} | T | \alpha, \vec{k} \rangle\rangle$ can differ from zero only if the ejected electron is in a σ state, with $\mu_\alpha = \Lambda_\alpha - \Lambda_f$ equal to zero. This restricts the electronic transitions to those for which the projection quantum numbers $\Lambda_f(\text{Na}_2^+)$ and $\Lambda_\alpha(\text{Na}_2)$ are equal to one another.

From the first, second, and fifth of these rules one concludes (see Appendix) that the quantity $\sigma_{\alpha'\alpha''}(E)$, defined by Eq. (7), can be different from zero only if the two ABO initial states α' and α'' have the same quantum numbers for electron spin and for the axial projection of electronic orbital angular momentum. As we soon shall see (in Sec. III), these restrictions eliminate virtually all off-diagonal contributions from the cross-section formula (6). It should be recognized that the three rules which cause so many off-diagonal elements $\sigma_{\alpha'\alpha''}(E)$ to vanish depend in no way upon integration over the momentum variable \vec{k} or summation over the indices $\vec{\epsilon} = (\epsilon, \hat{\epsilon})$ and f . The conclusions we have reached are equally applicable to electron-energy and electron-angle differential cross sections and to cross sections specific to the production of ions in single rovibronic states.

It is shown in the Appendix that integration over the direction of motion $\hat{\epsilon}$ of the ejected electron introduces an additional restriction on the quantities $\sigma_{\alpha'\alpha''}(E)$, namely, that the parities of the two states α' and α'' be identical. Thus, $\sigma_{\alpha'\alpha''}(E)$ is zero unless the two ABO states belong to the same irreducible representation of the homonuclear diatomic group $D_{\infty h}$ and have the same electron-spin quantum numbers.

In addition to the dynamic variables $\sigma_{\alpha'\alpha''}(E)$, the formula for the cross section involves matrix elements of the electronic density operator associated with the laser-prepared initial state. It is through these matrix elements that the cross section $\sigma(E, \beta)$ depends upon β , the angle between the axes of the beam and of the laser polarization. This β dependence of $\langle\alpha' | \rho_{\text{el}} | \alpha''\rangle$ resides in the quantities $\langle\alpha' | M_A, M_B \rangle$ and $\langle M_A, M_B | \alpha''\rangle$ which connect the ABO states $|\alpha'\rangle$ and $|\alpha''\rangle$ to the atomic states $|M_A, M_B\rangle$. The atomic states are associated with the laser frame of reference whereas the ABO states are referred to a molecular frame, the polar axis of which is in asymptotic coincidence (prior to collision) with the direction of relative motion and so also with the direction of the effusive beam.

In order to compute the coupling coefficients $\langle\alpha | M_A, M_B \rangle$ the two sets of electronic states must be referred to a common frame of reference. This can be accomplished by expressing the individual laser-frame atomic states $|J_j, M_j\rangle$ in terms of their molecular-frame coun-

terparts $|J_j, \Omega_j\rangle$ according to the relationship

$$|J_j, M_j\rangle = \sum_{\Omega_j} |J_j, \Omega_j\rangle \mathcal{R}_{\Omega_j M_j}^{(J_j)}(\beta). \quad (11)$$

Here $\mathcal{R}_{\Omega M}^{(J)}(\beta) \equiv \mathcal{R}_{\Omega M}^{(J)}(0, \beta, 0)$ is a representation coefficient of the three-dimensional rotation group, as defined by Messiah.¹¹ The pair states in the two frames are then connected by the formula

$$|M_A, M_B\rangle = \sum_{\Omega_A, \Omega_B} |\Omega_A, \Omega_B\rangle \mathcal{R}_{\Omega_A M_A}^{(J_A)}(\beta) \mathcal{R}_{\Omega_B M_B}^{(J_B)}(\beta) \quad (12)$$

and the matrix elements of the electronic density operator can be written in the forms

$$\begin{aligned} \langle\alpha' | \rho_{\text{el}} | \alpha''\rangle &= \sum_{\substack{\Omega'_A, \Omega'_B, \\ \Omega''_A, \Omega''_B}} \langle\alpha' | \Omega'_A, \Omega'_B\rangle P_{\Omega'_A, \Omega'_B}^{(J_A)}(\beta) \\ &\quad \times P_{\Omega''_B, \Omega''_A}^{(J_B)}(\beta) \langle\Omega''_A, \Omega''_B | \alpha''\rangle \end{aligned} \quad (13)$$

with

$$P_{\Omega'_j, \Omega''_j}^{(J_j)}(\beta) = \sum_{M_j} p_j(M_j) \mathcal{R}_{\Omega'_j M_j}^{(J_j)}(\beta) \mathcal{R}_{\Omega''_j M_j}^{(J_j)*}(\beta). \quad (14)$$

As a final step, the eigenstates $|J_j, \Omega_j\rangle$ of total angular momentum can be connected to the (molecular-frame) eigenstates of orbital and spin angular momentum, $|L_j, S_j, \Omega_j, \Sigma_j\rangle = |L_j, \Lambda_j\rangle |S_j, \Sigma_j\rangle$, by the vector coupling relationships

$$\begin{aligned} |J_j, \Omega_j\rangle &= |J_j, \Omega_j(L_j, S_j)\rangle \\ &= \sum_{\Lambda_j, \Sigma_j} \langle L_j, S_j, \Lambda_j, \Sigma_j | J_j, \Omega_j\rangle |L_j, S_j, \Lambda_j, \Sigma_j\rangle. \end{aligned} \quad (15)$$

The molecular-frame coupling coefficients which occur in Eq. (13) then can be written in the computationally convenient forms

$$\begin{aligned} \langle\alpha | \Omega_A, \Omega_B\rangle &= \sum_{\substack{\Lambda_A, \Lambda_B, \\ \Sigma_A, \Sigma_B}} \langle\alpha | \Lambda_A, \Sigma_A, \Lambda_B, \Sigma_B\rangle \\ &\quad \times \langle L_A, S_A, \Lambda_A, \Sigma_A | J_A, \Omega_A\rangle \\ &\quad \times \langle L_B, S_B, \Lambda_B, \Sigma_B | J_B, \Omega_B\rangle. \end{aligned} \quad (16)$$

This completes the formal theory. The integral cross section for AI has been expressed in terms of two sets of quantities, one involving matrix elements of the transition operator, the other consisting of matrix elements of the density operator representative of the laser-prepared initial state. From a detailed examination of the electronic and nuclear dynamics we have obtained strong symmetry restrictions on the members of the first of these two sets.

The construction of the density matrix has been reduced to a tedious but routine task requiring nothing beyond the evaluation of sums containing vector-coupling coefficients and representation coefficients of the three-dimensional rotational group. In Sec. III this theoretical machinery will be used to analyze the AI experiments of Kircz, Morgenstern, and Nienhuis.

III. APPLICATION TO THE KMN EXPERIMENT

We label each electronic state of Na_2 with its term symbol and the dominant configuration near the united atom limit of $R=0$. Thus, the lowest of the ${}^1\Sigma_g^+$ states depicted in Fig. 1 is labeled ${}^1\Sigma_g^+(\sigma_g^2)$. The beam temperature in the KMN experiment was approximately 300°C , corresponding to a mean kinetic energy of relative motion equal to 0.05 a.u. Therefore, the (Franck-Condon) selection rule, (iv) of Sec. II, eliminates from consideration all states with potential-energy curves which intersect the curve for $\text{Na}_2^+(X^2\Sigma_g^+)$ at energies much in excess of the $\text{Na}(3p)\text{-Na}(3p)$ asymptotic level of 0.149 a.u., cf. Fig. 1. It is expected that states dominated by configurations with one or more antibonding (valence) orbitals will have steeply repulsive potential-energy curves. We assume that these states do not contribute to the experimentally observed rate of AI. Those which remain are listed in Table I. They appear to be the only possible contributors to the rate of AI measured by Kircz, Morgenstern, and Nienhuis. The assignments of dominant configurations at small R have been made by assuming that none of these states experience avoided crossings.

From the selection rules of the preceding section it is easily verified that all off-diagonal elements of $\sigma_{\alpha'\alpha''}(E)$, $\alpha' \neq \alpha''$, are zero for the states listed in Table I, with the possible exception of $\sigma_{AB}(E)$. Thus, the integral cross section can be written as

$$\sigma(E, \beta) = \sum_{\alpha} \sigma_{\alpha\alpha}(E) \langle \alpha | \rho_{\text{el}} | \alpha \rangle + 2\text{Re}[\sigma_{AB}(E) \langle A | \rho_{\text{el}} | B \rangle], \quad (17)$$

with the summation extending over the states of Table I.

Although the symmetries of the A and B states are the same, they are composed from disjoint sets of σ and π or-

bitals, respectively (or, equivalently, from $3p$ atomic orbitals with $M_L=0$ and ± 1 , respectively). Because of this the matrix element $\langle A | \rho_{\text{el}} | B \rangle$ vanishes and $\sigma(E, \beta)$ given by Eq. (18) reduces to a weighted sum of cross sections $\sigma_{\alpha\alpha}(E)$, each of which is specific to the AI of a single ABO initial state. The weighting factors in this sum are the populations of the ABO states in the laser-prepared beam. These diagonal elements of the electronic density matrix can be evaluated using Eqs. (13), (14), and (16). The results are as follows:

$$\begin{aligned} \langle A | \rho_{\text{el}} | A \rangle &= \frac{2}{9}b^2, \\ \langle B | \rho_{\text{el}} | B \rangle &= \frac{1}{2}a^2 + \frac{1}{36}b^2 + \sqrt{2}/6(c^2 - d^2), \\ \langle C^{\pm 1} | \rho_{\text{el}} | C^{\pm 1} \rangle &= \frac{1}{3}ab + \frac{1}{9}b^2 - \frac{1}{3}d^2, \\ \langle D(\pm 1) | \rho_{\text{el}} | D(\pm 1) \rangle &= \frac{1}{3}(ab + d^2), \\ \langle D(0) | \rho_{\text{el}} | D(0) \rangle &= \frac{1}{2}a^2 + \frac{1}{36}b^2 - (\sqrt{2}/6)(c^2 - d^2), \\ \langle E^{+1}(+1) | \rho_{\text{el}} | E^{+1}(+1) \rangle &= \langle E^{-1}(-1) | \rho_{\text{el}} | E^{-1}(-1) \rangle \\ &= \frac{2}{3}(ab - c^2), \\ \langle E^{+1}(-1) | \rho_{\text{el}} | E^{+1}(-1) \rangle &= \langle E^{-1}(+1) | \rho_{\text{el}} | E^{-1}(+1) \rangle \\ &= \frac{1}{9}b^2, \\ \langle E^{\pm 1}(0) | \rho_{\text{el}} | E^{\pm 1}(0) \rangle &= \frac{1}{3}ab + \frac{1}{9}b^2 - \frac{1}{3}d^2, \end{aligned} \quad (18)$$

with

$$\begin{aligned} a &= \frac{1}{12} + \frac{1}{4}\sin^2\beta, \\ b &= \frac{5}{12} - \frac{1}{4}\sin^2\beta, \\ c &= -(\sqrt{3}/6)\sin\beta\cos\beta, \\ d &= (\sqrt{3}/12)\sin^2\beta. \end{aligned} \quad (19)$$

The single-state cross sections $\sigma_{\alpha\alpha}(E)$ depend neither upon the algebraic sign of the projection quantum number for electronic orbital angular momentum nor upon the projection quantum number of electron spin. Thus, for example, $\sigma_{C^+C^+} = \sigma_{C^-C^-} \equiv \sigma_{CC}$ and $\sigma_{D(0)D(0)} = \sigma_{D(1)D(1)} = \sigma_{D(-1)D(-1)} \equiv \sigma_{DD}$. Therefore, by combining Eqs. (17) and (18) we obtain the final working formula

TABLE I. Several ABO states of Na_2^+ which correlate asymptotically with the separated atom configuration $\text{Na}(3p)\text{-Na}(3p)$. The states included in this table are those with dominant configurations at small internuclear separations which do not include antibonding valence orbitals. The superscripts ± 1 of π orbitals and Π states refer to the projection quantum numbers of orbital angular momentum. The symbols $D(\Sigma)$ and $E^{\pm 1}(\Sigma)$ with $\Sigma=0, \pm 1$ indicate the components of a spin triplet.

ABO states α	Dominant configuration at small R	Orbital form as $R \rightarrow \infty$
$A \equiv {}^1\Sigma_g^+(\sigma_g^2)$	σ_g^2	$\sigma_g^2 - \sigma_u^2$
$B \equiv {}^1\Sigma_g^+(\pi_u^1\pi_u^{-1})$	$\pi_u^1\pi_u^{-1}$	$\pi_u^1\pi_u^{-1} - \pi_g^1\pi_g^{-1}$
$C^{\pm 1} \equiv {}^1\Pi_u(\sigma_g\pi_u^{\pm 1})$	$\sigma_g\pi_u^{\pm 1}$	$\sigma_g\pi_u^{\pm 1} - \sigma_u\pi_g^{\pm 1}$
$D(\Sigma) \equiv {}^3\Sigma_g^-(\pi_u^1\pi_u^{-1})$	$\pi_u^1\pi_u^{-1}$	$\pi_u^1\pi_u^{-1} - \pi_g^1\pi_g^{-1}$
$E^{\pm 1}(\Sigma) \equiv {}^3\Pi_u(\sigma_g\pi_u^{\pm 1})$	$\sigma_g\pi_u^{\pm 1}$	$\sigma_g\pi_u^{\pm 1} - \sigma_u\pi_g^{\pm 1}$

$$\begin{aligned} \sigma(E, \beta) = & \left(\frac{2}{9}b^2\right)\sigma_{AA}(E) + \left[\frac{1}{2}a^2 + \frac{1}{36}b^2 + (\sqrt{2}/6)(c^2 - d^2)\right]\sigma_{BB}(E) + \left[2\left(\frac{1}{3}ab + \frac{1}{9}b^2 - \frac{1}{3}d^2\right)\right]\sigma_{CC}(E) \\ & + \left\{2\left[\frac{1}{3}(ab - d^2)\right] + \left[\frac{1}{2}a^2 + \frac{1}{36}b^2 - (\sqrt{2}/6)(c^2 - d^2)\right]\right\}\sigma_{DD}(E) \\ & + \left\{2\left[\frac{2}{3}(ab - c^2)\right] + 2\left(\frac{1}{9}b^2\right) + 2\left(\frac{1}{3}ab + \frac{1}{9}b^2 - \frac{1}{3}d^2\right)\right\}\sigma_{EE}(E). \end{aligned} \quad (20)$$

It is convenient to deal with the dimensionless cross section

$$\sigma^*(E, \beta) \equiv \sigma(E, \beta) / \sigma(E, 0) \quad (21)$$

instead of with $\sigma(E, \beta)$ itself. We have plotted separately in Fig. 3 each of the five reduced cross sections $\sigma_{\alpha\alpha}^*(E, \beta)$ specific to the individual states $\alpha = A, B, C, D$, and E , e.g., $\sigma_{AA}^*(E, \beta) = [b(\beta)]^2 / [b(0)]^2$. It is obvious that no single ABO state can account for the experimental data. Thus, there must be at least two contributing ABO states to the integral cross section for AI.

We fit the theoretical formula $\sigma^*(E, \beta)$ to the measured cross section $\sigma_{\text{exp}}^*(E, \beta)$ of KMN by adjusting the values of the single-state integral cross sections $\sigma_{\alpha\alpha}(E)$. The fitting is done subject to the restriction that $\sigma^*(E, \pi/2) = 0.605$. This condition is imposed for convenience and justified by the large amount of experimental data near $\beta = \pi/2$. $\sigma_{\text{exp}}(E, \beta)$ is less precisely known for other values of β . We accommodate to this by introducing the squared mean error

$$\langle \epsilon^2 \rangle = \frac{2}{\pi} \int_0^{\pi/2} d\beta [\sigma^*(E, \beta) - \sigma_{\text{exp}}^*(E, \beta)]^2 \quad (22)$$

and then determining values of the set $\{\sigma_{\alpha\alpha}(E); \alpha = A, B, C, D, E\}$ of single-state integral cross sections for which the rms error $100 \langle \epsilon^2 \rangle^{1/2}$ is 5% or less. This procedure generates a number of fits from which the following conclusions can be drawn.

(i) The dominant contributor is the A state [$^1\Sigma_u^+(\sigma_g^2)$]. Thus, the value of σ_{AA} typically is found to be three times larger than the sum of σ_{BB} [$^1\Sigma_g^+(\pi_u^2)$] and σ_{DD} [$^3\Sigma_g^-(\pi_u^2)$] and six times greater than the sum of σ_{CC} [$^1\Pi_u(\sigma_g\pi_u)$] and σ_{EE} [$^3\Pi_u(\sigma_g\pi_u)$].

(ii) It is difficult to separate the contributions of the B [$^1\Sigma_g^+(\pi_u^2)$] and D [$^3\Sigma_g^-(\pi_u^2)$] states because (a) their combined contributions only amount to about 30% of that of the A state and (b) the associated components of the density operator have very similar angular dependences, cf. curves B and D of Fig. 3. However, there is little chance that both of these states are contributors to the experimentally observed rate of AI. The reason for this is the large level splitting (associated with exchange integrals with values on the order of 1 eV ≈ 0.074 a.u.) that will occur at small internuclear separations. The triplet D state will be the lower lying of the two and it very likely lies so low that its energy curve does not even intersect that for the Na_2^+ ground state. In this event the AI-active state would be the D state [$^1\Sigma_g^+(\pi_u^2)$].

Analogous statements apply to the paired C [$^1\Pi_u(\sigma_g\pi_u)$] and E [$^3\Pi_u(\sigma_g\pi_u)$] states. In this case the problem of determining separate contributions is even greater because their sum is so very small, namely, no greater than 15% of that of the A state, and possibly much less.

(iii) The best fit is obtained with $\sigma_{AA} \approx 23$, $\sigma_{CC} \approx \sigma_{EE} = 0$, and with B - and D -state cross sections conforming to the constraints $\sigma_{BB} \approx 8.97 - 2.13\sigma_{DD}$ and $4 > \sigma_{DD} > 2.5$.

In summary, our analysis indicates that at least two ABO states are participants in the experimentally observed AI process. The most reactive of these states is $X^1\Sigma_g^+(\sigma_g^2)$ and the next most reactive is either $^1\Sigma_g^+(\pi_u^2)$ or $^3\Sigma_g^-(\pi_u^2)$. Accurate electronic state calculations are needed in order to resolve the remaining uncertainties.

IV. CLOSING REMARKS

KMN and Nienhuis have analyzed the cross section for AI without reference to ABO states of the reactant atoms. They label elements of the transition operator with the quantum numbers J_j and M_j of individual atoms. Cross terms connecting reactant states with different labels of this sort are discarded without much justification beyond an implication that cancellation should occur because of averaging over experimentally uncontrolled (and/or uncontrollable) parameters. This should be contrasted with the cross terms of our theory which vanish identically regardless of whether one sums over the values of the final state variables \bar{k} , $\bar{\epsilon}$, and f .

Our preoccupation with the ABO states began with an awareness of the remarkably successful theories of AI (and the related Penning ionization process) which are based on these states.^{10,12} It seemed very likely to us that the results of experiments such as those of KMN could be related to cross sections specific to the AI of individual ABO states. Furthermore, it seemed reasonable to expect that coupling would be limited to interferences between reaction paths associated with different ABO states which were asymptotically degenerate and that the observable effects of these interferences would be washed out, except perhaps in differential scattering experiments. It has been a pleasant surprise to discover that there are additional, very fundamental reasons for the absence of (some) cross terms connecting the different ABO channels for AI.

Note added in proof. E. W. Rothe, R. Theyunni, G. P. Reck, and C. C. Tung [private communication (unpublished)] recently have repeated the KMN experiment and found *qualitatively different* results. Thus, in place of KMN's normalized cross section [cf. Eq. (12)]

$$\sigma^*(\text{KMN}) \approx (1/1.37)[1 + 0.27 \cos 2\beta + 0.10 \cos 4\beta]$$

they obtain

$$\sigma^*(\text{RTRT}) \approx (1/1.38)[1 + 0.38 \cos 4\beta].$$

The reason for this great discrepancy currently is unknown. Our method of analysis can be applied to this new set of data as well as to that of KMN. We shall communicate the implications of the RTRT experiments in the near future.

ACKNOWLEDGMENTS

This work was supported by a grant from the National Science Foundation. We are grateful to Professor D. G. Truhlar for correcting an error in our thinking; he is not responsible for others which may have gone undetected.

APPENDIX: SELECTION RULES OF $\sigma_{\alpha'\alpha''}(E)$

The transition matrix for associative ionization can be constructed from results presented in Saha, Dahler, and Nielsen's (SDN) recent paper¹³ on laser-induced chemi-ionization. Thus, from Eqs. (2.26), (3.9), (4.1), and (4.22) of SDN it follows that

$$\begin{aligned} \langle\langle E_{n'}^{L'}, \vec{\epsilon} | T | \alpha, \vec{k} \rangle\rangle &= \left[\frac{2L'+1}{4\pi} \right]^{1/2} \sum_{\lambda'} Y_{\lambda', -M'}(\hat{\epsilon}) \sum_L \frac{2L+1}{4\pi} i^L e^{i\bar{\eta}_\alpha^L} \langle F_f^{L'}(E_{n'}^{L'}) | V_{\epsilon\lambda'\mu_\alpha} | \bar{F}_\alpha^L(E) \rangle \\ &\times \sum_J (2J+1) \begin{bmatrix} L & L' & J \\ 0 & M' & -M' \end{bmatrix} \begin{bmatrix} L & L' & J \\ 0 & 0 & 0 \end{bmatrix} \\ &\times \int d\hat{R} [\mathcal{R}_{-M', 0}^{(J)}(\hat{R})]^* \mathcal{R}_{-M', \mu_\alpha}^{(\lambda')}(\hat{R}). \end{aligned} \quad (\text{A1})$$

This matrix element is specific to production of the diatomic ion in a state characterized by the set of quantum numbers $(n', L', M', \Lambda_f, p_f)$ and a free electron with the energy and direction of motion $\vec{\epsilon} = (\epsilon, \hat{\epsilon})$.

The phase shift $\bar{\eta}_\alpha^L$ and the radial wave functions $F_f^{L'}(E_{n'}^{L'} | R)$ and $\bar{F}_\alpha^L(E | R)$ are fully defined in Ref. 13. The spherical harmonics $Y_{\lambda', M'}(\hat{\epsilon})$ are referred to a laboratory frame of reference, the polar axis of which is parallel to the initial direction of relative motion of the two colliding atoms. $\mathcal{R}_{MM'}^{(L)}(\hat{R}) = \mathcal{R}_{MM'}^{(L)}(\phi, \theta, 0)$ is a representation coefficient of the three-dimensional rotation group, as defined by Messiah,¹¹ and $\hat{R}(d\hat{R} = \sin\theta d\theta d\phi)$ refers to the rotation which connects the laboratory and body-fixed frames of reference.

The function $V_{\epsilon\lambda'\mu_\alpha}(R)$ is the electronic matrix element

$$V_{\epsilon\lambda'\mu_\alpha}(R) = i^{-\lambda'} e^{i\sigma^\lambda} \langle \phi_{\epsilon\lambda'\mu_\alpha}^- | H_{el} | \phi_\alpha \rangle, \quad (\text{A2})$$

with σ^λ denoting the Coulomb wave shift. Here ϕ_α is the ABO wave function of a bound state of Na_2 , referred to the body-fixed frame. Associated with this state is an axial projection of the electronic orbital angular momentum equal to $\hbar\Lambda_\alpha$. $\phi_{\epsilon\lambda'\mu_\alpha}^-$ is an ABO function descriptive of (a) a diatomic ion with an electronic orbital angular momentum projection quantum number Λ_f and a parity p_f and (b) an unbound electron with energy ϵ , parity $p_e = (-1)^\lambda$, and orbital angular momentum projection quantum number $\mu_\alpha = \Lambda_\alpha - \Lambda_f$ (see Ref. 14 for details). The parity and projection quantum numbers of the state described by the wave function $\phi_{\epsilon\lambda'\mu_\alpha}^-$ are $p_f p_e$ and $\Lambda_f + \mu_\alpha$, respectively.

1. Parity selection rule

According to the definition (7) and the formula (A1),

$$\begin{aligned} \sigma_{\alpha'\alpha''}(E) &\propto \int d\hat{\epsilon} \langle\langle f, \vec{\epsilon} | T | \alpha', \vec{k} \rangle\rangle \langle\langle f, \vec{\epsilon} | T | \alpha'', \vec{k} \rangle\rangle^* \\ &\propto \sum_{\lambda', \lambda''} [\langle F_f^{L'}(E_{n'}^{L'}) | V_{\epsilon\lambda'\mu_\alpha} | \bar{F}_\alpha^L(E) \rangle \langle F_f^{L''}(E_{n'}^{L''}) | V_{\epsilon\lambda''\mu_\alpha} | \bar{F}_\alpha^{L''}(E) \rangle^*] \left[\int d\hat{\epsilon} Y_{\lambda', -M'}(\hat{\epsilon}) Y_{\lambda'', -M'}^*(\hat{\epsilon}) \right] (\dots). \end{aligned} \quad (\text{A3})$$

The integral over the direction of motion $\hat{\epsilon}$ of the ejected electron will be different from zero only if $\lambda'' = \lambda'$ and so the electronic matrix elements $V_{\epsilon\lambda'\mu_\alpha}$ and $V_{\epsilon\lambda''\mu_\alpha}$ appearing in (A3) connect the initial ABO states $\phi_{\alpha'}$ and $\phi_{\alpha''}$ to final states with a common value of parity equal to $p_f(-1)^{\lambda'}$. Consequently, $\sigma_{\alpha'\alpha''}(E)$ vanishes unless the parities of the α' and α'' states are identical.

2. Projection quantum number rule

We now assume that the relative angular momentum of the heavy particles is unaltered by the occurrence of the electronic transition. The mathematical consequences of this assumption are obtained by replacing $i^L \exp(i\bar{\eta}_\alpha^L) | \bar{F}_\alpha^L(E) \rangle$ with $i^{L'} \exp(i\bar{\eta}_\alpha^{L'}) | \bar{F}_\alpha^{L'}(E) \rangle$ in Eq. (A1), which then reduces to

$$\langle\langle E_{n'}^{L'}, \vec{\epsilon} | T | \alpha, \vec{k} \rangle\rangle = \left[\frac{2L'+1}{4\pi} \right]^{1/2} i^{L'} e^{i\bar{\eta}_\alpha^{L'}} \sum_{\lambda'} Y_{\lambda', 0}(\hat{\epsilon}) \langle F_f^{L'}(E_{n'}^{L'}) | V_{\epsilon\lambda'\mu_\alpha} | \bar{F}_\alpha^{L'}(E) \rangle \sum_J \frac{2J+1}{4\pi} \int d\hat{R} [\mathcal{R}_{0,0}^{(J)}(\hat{R})]^* \mathcal{R}_{0,\mu_\alpha}^{(\lambda')}(\hat{R}). \quad (\text{A4})$$

To evaluate the integral appearing at the end of this formula we use the addition theorem for the representation coefficients (Messiah,⁸ C.69) together with a few other relationships (Messiah, C.66, C.80b, and B.93) and obtain the expression

$$\sum_J \frac{2J+1}{4\pi} \int d\hat{R} [\mathcal{R}_{0,0}^{(J)}(R)]^* \mathcal{R}_{0,\mu_\alpha}^{(\lambda')}(\hat{R}) = \sum_K \left[\frac{2K+1}{4\pi} \left(\frac{(K-\mu_\alpha)!}{(K+\mu_\alpha)!} \right)^{1/2} 2\pi \int_{-1}^1 dx P_K^{\mu_\alpha}(x) \right] \times \left[\sum_J (2J+1) \begin{Bmatrix} J & \lambda' & K \\ 0 & 0 & 0 \end{Bmatrix} \begin{Bmatrix} J & \lambda' & K \\ 0 & \mu_\alpha & -\mu_\alpha \end{Bmatrix} \right]. \quad (\text{A5})$$

According to C.15b of Messiah the last factor in (A5) is equal to $\delta_{\mu_\alpha,0}$. With μ_α set equal to zero the first factor is $\delta_{K,0}$ and so the entire expression equals $\delta_{\mu_\alpha,0}$. Consequently, (A4) reduces to

$$\langle\langle E_n^{L'}, \vec{\epsilon} | T | \alpha, \vec{k} \rangle\rangle = \delta_{\Lambda_\alpha, \Lambda_f} \left[\frac{2L'+1}{4\pi} \right]^{1/2} i^{L'} e^{i\eta_\alpha^{L'}} \sum_{\lambda'} Y_{\lambda',0}(\hat{\epsilon}) \langle F_f^{L'}(E_n^{L'}) | V_{\epsilon\lambda',0} | \bar{F}_\alpha^{L'}(E) \rangle. \quad (\text{A6})$$

This is the result referred to in the text as selection rule (v). What we have proved is that *if* the relative angular momentum of the heavy particles does not change as a consequence of the electronic transition, then the only electronic transitions that can occur are those for which the electronic orbital angular momentum projection quantum number of the reactant (Na-Na) state is equal to that of the product Na_2^+ ion.

Although we have not yet found a proof, it seems likely that the equality of L and L' (or equivalently, of Λ_f and Λ_α) can be established, not as an exact selection rule, but as a (Franck-Condon) propensity rule. The equality of Λ_α and Λ_f has been assumed as a simplifying approximation in a number of studies of associative and Penning ionization.^{10,12} The semiquantitative successes of these calculations could be construed as evidence in support of the approximation.

The quantity defined by Eq. (A5)—and shown here to

equal $\delta_{\mu_\alpha,0}$ —appears in SDN's theory of laser-induced chemi-ionization¹³ and also in Saha, Dahler, and Jones's (SDJ) recent paper¹⁵ on laser-induced excitation transfer. Specifically, the quantity $A_m(\lambda | m')$ defined by Eq. (4.20) of SDN now can be identified as being equal to $\delta_{\mu_\alpha,0} \delta_{m',m}$. As a consequence of this, SDN's Eq. (4.19) becomes

$$\bar{T}_{m'}(E'L', EL', \epsilon\lambda; \omega) = \delta_{\mu_\alpha,0} \bar{T}(E'L', EL', \epsilon\lambda - m'; \omega), \quad (\text{A7})$$

the conclusion being that the transition matrix $T(\vec{E}', \vec{\epsilon} | \vec{E})$ for laser-induced Penning ionization differs from zero only if $\Lambda_f(AB^+) = \Lambda_i(AB)$. Similar considerations apply to SDN's theory of laser-induced associative ionization. Finally, the quantity u_μ defined by Eq. (2.16) of SDJ now can be seen to equal $4\pi\delta_{\mu,0}$.

¹A. de Jong and F. van der Valk, *J. Phys. B* **12**, L561 (1979).

²G. H. Bearman and J. J. Leventhal, *Phys. Rev. Lett.* **41**, 1227 (1978).

³V. S. Kushawaha and J. J. Leventhal, *Phys. Rev. A* **22**, 2468 (1980).

⁴R. Bonanno, J. Boulmer, and J. Weiner, *Phys. Rev. A* **28**, 604 (1983).

⁵J. G. Kircz, R. Morgenstern, and G. Nienhuis, *Phys. Rev. Lett.* **48**, 610 (1982).

⁶R. Montagnani, P. Riani, and Oriano Salvetti, *Theor. Chim. Acta* **64**, 431 (1984). Here, the label $X^1\Sigma_g^+$ refers to the lowest lying $^1\Sigma_g^+$ state which correlates to the asymptotic state $\text{Na}(^2P) + \text{Na}(^2P)$.

⁷G. Nienhuis, *Phys. Rev. A* **26**, 3137 (1982).

⁸A. Messiah, *Quantum Mechanics* (Wiley, New York, 1962); see Eqs. XIX.113–XIX.115 and XVII.52.

⁹Our general formalism is equally applicable to experimental situations such as those envisioned by A. E. Orel and K. C. Kulander, *J. Chem. Phys.* **79**, 1326 (1983), who have presented a classical-path, impact-parameter theory of charge exchange involving atomic states coherently excited (nondiagonal electronic density matrix) by a very brief pulse of laser radiation.

¹⁰R. J. Bieniek, *Phys. Rev. A* **18**, 392 (1978); see also W. H. Miller, C. A. Slocumb, and H. F. Schaeffer III, *J. Chem. Phys.* **56**, 1347 (1972); J. N. Bardsley, *J. Phys. B* **1**, 349 (1968).

¹¹Appendix C of Ref. 8.

¹²A. P. Hickman and H. Morgner, *J. Phys. B* **9**, 1765 (1976).

¹³H. P. Saha, J. S. Dahler, and S. E. Nielsen, *Phys. Rev. A* **28**, 1487 (1983).

¹⁴H. P. Saha and J. S. Dahler, *Phys. Rev. A* **28**, 2859 (1983).

¹⁵H. P. Saha, J. S. Dahler, and D. M. Jones, *Phys. Rev. A* **30**, 1345 (1984).